2013

Polypyrrole stretchable actuators

Wen Zheng
University of Wollongong, wenz@uow.edu.au

Gursel Alici
University of Wollongong, gursel@uow.edu.au

Phillip R. Clingan
University of Wollongong, philipc@uow.edu.au

Bridget Munro
University of Wollongong, bmunro@uow.edu.au

Geoffrey M. Spinks
University of Wollongong, gspinks@uow.edu.au

See next page for additional authors

Polypyrrole stretchable actuators

Abstract

Here, we report a simple way to prepare stretchable polypyrrole (PPy)-based actuator materials that can be operated over a wide dynamic strain range and generate useable actuation displacements and pressures. The stretchable actuators were prepared as a laminated composite of PPy and a gold-coated roughened rubber sheet. By manipulating the corrugated surface of the rubber substrate, the stretchability of PPy was greatly improved. Gold-coated rubbers could be stretched to 30 percent without significant change in electrical resistance. The corrugated PPy/gold/rubber laminates successfully showed - 1 percents of actuation strain even when prestretched to 24 percent. The actuation strains were smaller than for similar free-standing PPy films and a detailed analysis of the effects of corrugation and of the rubber substrate are presented to predict actuation strain under various prestretch strains.

Keywords

actuators, stretchable, polypyrrole

Disciplines

Engineering | Physical Sciences and Mathematics

Publication Details

Zheng, W., Alici, G., Clingan, P. R., Munro, B., Spinks, G. M., Steele, J. R. & Wallace, G. G. (2013). Polypyrrole stretchable actuators. Journal of Polymer Science, Part B: Polymer Physics, 51 (1), 57-63.

Authors

Wen Zheng, Gursel Alici, Phillip R. Clingan, Bridget Munro, Geoffrey M. Spinks, Julie R. Steele, and Gordon G. Wallace

Polypyrrole Stretchable Actuators

Wen Zheng[1], Gursel Alici[2], Philip R Clingan[3], Bridget J Munro[1,4], Geoffrey M Spinks[1]*, Julie R Steele[4] and Gordon G Wallace[1]

[1] Intelligent Polymer Research Institute, ARC center of Excellence for Electromaterials Science, AIIM Facility, Innovation Campus, University of Wollongong, Wollongong, NSW, 2522, Australia.

[2]School of Mechanical, Materials, and Mechatronic Engineering, University of Wollongong, Northfields Avenue, Wollongong, NSW, 2522, Australia.

[3]Illawarra Health and Medical Research Institute, University of Wollongong, Northfields Avenue, Wollongong, NSW, 2522, Australia.

[4] Biomechanics Research Laboratory, School of Health Sciences, University of Wollongong, Northfields Avenue, Wollongong, NSW, 2522, Australia.

Correspondence to: Geoffrey M Spinks (E-mail: *gspinks@uow.edu.au*)

(Additional Supporting Information may be found in the online version of this article.)

ABSTRACT

Here we report a simple way to prepare stretchable polypyrrole (PPy) based actuator materials that can be operated over a wide dynamic strain range and generate useable actuation displacements and pressures. The stretchable actuators were prepared as a laminated composite of polypyrrole and a gold-coated roughened rubber sheet. By manipulating the corrugated surface of the rubber substrate, the stretchability of PPy was greatly improved. Gold-coated rubbers could be stretched to 30% without significant change in electrical resistance. The corrugated PPy/gold/rubber laminates successfully showed ~1% of actuation strain even when pre-stretched to 24%. The actuation strains were smaller than for similar free-standing PPy films and a detailed analysis of the effects of corrugation and of the rubber substrate are presented to predict actuation strain under various pre-stretch strains.

KEYWORDS conducting polymers, polypyrrole, wearable electronics, stretchable actuator, lymphedema sleeve.

INTRODUCTION

Wearable actuators are potentially useful in assisting or enhancing human movement. They can be used, for example, in exoskeletons for training,[1] therapy,[2] and assisting with functional activities of daily living.[3, 4] Such devices, however, have to be compact, robust, lightweight and offer a suitable interface between the device and the operator's soft tissues, as well as provide easy control strategies. Wearable actuators also require stretchable electronics where the circuit can sustain large deformations without electrical failure or detrimental loss of performance.[5-7] The property requirements for stretchable electronics vary depending upon the final application. For example, 10 to ~30% of strain is reported to be needed for stretchable displays,[8] ~20% for flexible solar cells,[9] ~120% for super capacitors,[10] and ~100% for batteries[11] and dielectric elastomer actuators.[12] In each case, the strain should occur without significant mechanical or electrical failure.

It is desirable to fabricate stretchable electronic circuits with the highest conductivity possible in order to reduce resistance losses and maximize performance. However, most good electrical conductors, like metal, silicon, or carbon nanotubes (CNTs), are very stiff and not stretchable. Typical free standing thin metal films can fracture at tensile strain below 1%.[13] The strategy of fabricating stretchable electronic substrates is to ensure that the conductor materials maintain a low strain and avoid damage during stretching. To realize such a strategy, it is typical to use an elastomer as a substrate and thin conductor coatings. Elastomer substrates allow reversible deformation to high strain, and are well suited to stretchable, bendable and roll-up electronics. To provide high stretchability in the conducting material a patterned metal/elastomer bilayer composite is commonly used.[14, 15] Corrugated structures provide extra tolerance during stretching and hence the electrical connection will remain even

to strains of tens of percent. Corrugated structures can be realized by releasing a pre-stretched metal coated elastomeric substrate.[16, 17] Wrinkles form spontaneously after removing external stress due to the mismatching elastic modulus between the metal and substrate. Those self-generated, randomly formed or non-optimized wavy structures can usually accommodate a strain of 20 to ~30% without electrical degradation.[17, 18] Some more carefully engineered corrugated shaped structures even allow strain of up to 100% without loss of conductivity.[5]

Conducting polymers (CPs), such as polypyrrole (PPy), have also been used as stretchable electronics. PPy coated onto stretchable fabrics, for example, has been shown to be robust and give a repeatable, linear resistance change when stretched. These PPy-coated conducting fabrics are ideal as strain sensors for monitoring human movement.[19-21] CPs are also widely studied as actuators,[22] although no stretchable CP actuators have been produced to date. Stretchable dielectric elastomer actuators are widely studied,[23] but their high input voltages preclude some applications. CP actuators offer the advantage of low voltage operation, easy control, large strain and high strength.[24] However, using PPy as stretchable actuators raises some challenges whereby a real device must accommodate large strains without failure or deterioration of performance. Free standing PPy is not very stretchable[25] and becomes even more brittle in its wet state than its dry state. For instance, dry state PPy free standing films break at ~100 MPa,[26] whereas solution saturated films fail at ~10 MPa.[27] Additionally, the maximum working stress is limited to less than half of the tensile strength.[22] Considering the elastic modulus of PPy is between tens and hundreds of mega Pascal,[28] the corresponding maximum strain of free standing films under those stresses is limited to less than 10%.

The present study considers whether corrugated PPy can operate as a stretchable actuator capable of working at high pre-loading strains and accommodate a large dynamic

strain range. Here we report a simple way to fabricate corrugated PPy/rubber bilayer substrates. The rubber provides a stretchable substrate and the corrugated PPy is the functional actuator material. One potential application of these stretchable actuators is a wearable garment to provide relief from lymphedema, which is a condition commonly seen in breast cancer survivors and usually causes swelling of arms and legs.[29] The wearable sleeve is a garment used to help 'massage' the limb to move lymphedema fluid back to the body's lymph system.[30]

EXPERIMENTAL

Reagents

Bis-trifluoromethanesulfonimide lithium (Li.TFSI) salt was purchased from Fluka and propylene carbonate (PC) was obtained from Sigma. Pyrrole monomer, also obtained from Fluka, was distilled before use. Waterproof silicon carbide sandpaper (Kwang Myung Abrasive Co., Ltd, South Korea) with different grit sizes was used as a moulding template to create rubber sheets with varied roughness. Liquid latex was used directly after being received from A.A.Rubber & Seals Pty, Ltd (Belmore, NSW, Australia).

Sample Preparation

Sandpaper (P120, P240, P600, P1200) was dipped into diluted liquid rubber (80% in water by weight) and then cured at 40°C overnight. The rubber sheets could be easily peeled off the sandpaper such that the surface roughness was set by the sand paper grit size. The roughened side of the rubber sheet was sequentially coated with 40 nm thick gold by sputtering and then PPy deposited at -31°C, 0.1 mA/cm^2 for 12 hours by a galvanostatic electropolymerization. The fabrication steps are illustrated in Figure 1.

Actuator Testing

Actuation tests for PPy/rubber samples were performed in 0.1 M Li.TFSI/PC electrolyte using a conventional three electrode set-up. A reticulated vitreous carbon foam counter electrode and $Ag|Ag^+$ reference electrode were used. Tests were performed either on free-standing sheets in an isotonic (constant tensile force) mode or isometrically with the rubber sheet wrapped tightly around a solid cylinder. During the isotonic actuation tests, when potential was applied, the change in length at a fixed applied force was measured by a lever arm dual mode force/distance transducer (305B, Aurora Scientific). The actuation strain was first measured at the lowest stress (based on the entire film thickness of ~1 kPa), and then the load was increased stepwise and the actuation test repeated at each load increment. This process was repeated until failure of the sample occurred.

To check the pressure generated under isometric conditions, a PPy/gold/rubber band (PPy surface towards the outside) was wrapped around a solid cylinder using low tension and joined securely at its ends. The wrapped cylinder was immersed in an electrolyte and a voltage step from -0.5 V to 0.5 V vs $Ag|Ag^+$ with 0.2 Hz scan frequency was applied to the system. During actuation, pressure changes were measured by a flexible pressure sensor (FlexiForce® Tekscan), which was embedded between the rubber and the solid cylinder. The diameter of the cylinder was ~38 mm.

Scanning electron microscopy (SEM) was performed with a JEOL JSM-7500 FA. Samples were frozen in liquid nitrogen and then cut for cross section inspection. Mechanical properties of the samples were measured using a Shimadzu Compact Tabletop Testing Machine. The average elastic modulus of the latex rubber band was 0.64±0.06 MPa (fitted from strain less than 50%). The *in situ* conductivity was measured with an Agilent 34410A

digital multimeter during sample stretching. The sample size for these tensile tests was 5 mm (width) x 20 mm (length) and a crosshead speed of 20 mm/min was used.

RESULTS AND DISCUSSION

Gold coated (gilt) rubber (sandpaper side) with and without PPy were inspected by SEM and are presented in Figure 2. Disordered surface features cover the entire surface of all samples. The degree of roughness was strongly correlated with grit size of the sandpaper. Cross section images of the PPy/gold/rubber were also examined (Figure 3). Generally, the PPy was found to grow following the surface undulations of the substrate, forming a corrugated structure. The average size, wavelength, and amplitude of surface asperities on the rubber generally matched the corresponding grit size, also shown in Figure 3. Adhesion of the gold/PPy to the rubber was reduced for the smoothest rubber films leading to delamination during sample drying and sectioning (Figure 3).

Metallic coatings and inter-connects for CP devices have been shown to improve performance as a significant voltage (*iR*) drop exists over millimetre dimensions in CP materials.[31] For this reason the substrate conductivity during stretching was initially checked. There was no obvious initial conductivity difference between the gold-coated rubber sheets prepared with different surface roughness. The average conductivity was measured as 1.3×10^{4} S/cm. Gilt rubbers with grit sizes of P1200, P600, P240 and P120 retained electrical continuity and showed negligible change in resistance when stretched to ~12%, ~18%, ~24% and 30%, respectively (Figure 4a). Above these strain limits the film resistance increased sharply. Gilt rubber from finer grit size sandpaper began to lose electrical conductivity at lower strain. The resistance increase at higher strains is associated with the formation and growth of cracks across the metal layer.[17] Recent studies have also found that chemical vapour deposited PPy on pre-stretched rubber with a similar corrugated structure can survive

to approximately 50% strain without breaking.[21] Ideally, if the corrugation direction is oriented, the electronic conductivity will remain almost unchanged until the surface roughness is flattened by stretching. Further stretching would then lead to complete metal rupture and loss of electrical continuity.

The actuation performance of various PPy/gold/rubber samples was tested at different applied loads (Figure 4c) and also at constant length (Figure 4d). The linear actuation strain decreased for all samples with increasing applied isotonic stress produced by applying a given pre-strain prior to actuation. Extrapolation of these data to zero applied stress gives the 'free strain' and it is seen that the free strain decreased from ~3% to ~1% as the rubber roughness increased. The pressure generated at fixed strain also decreased for the rougher rubber substrates. Corrugated free-standing PPy films have previously been shown to actuate to 12% linear strain under similar conditions at small applied stress.[32] By choosing proper dopant and solvent, the linear strain of PPy films can reach as high as 30%.[33] The smaller strains observed in the current study are likely due to a combination of the effect of corrugation, choice of dopant and the restricting effect of the rubber substrate.

A simple geometry model of the corrugated PPy provides a partial explanation for the decreased actuation observed for rougher rubber substrates (Figure S2 a). The length change projected on the axis parallel to the sheet direction is $l_o - \sqrt{(1+\varepsilon)^2(H^2 + l_o^2) - H^2}$ giving an actuation strain ε' of corrugated PPy as:

$$\varepsilon' = 1 - \sqrt{(1+\varepsilon)^2 + \frac{H^2}{l_o^2}(\varepsilon^2 + 2\varepsilon)} \quad \ldots\ldots \text{(a)}$$

where l_o is the unloaded sample length, *H* is a parameter related to the sample roughness (20-120 μm, Fig. 3) and ε is the actuation strain expected from non-corrugated PPy. Increasing

corrugation is expected to decrease the actuation strain in the sheet direction, as experimentally observed and shown schematically (Figure S2 b). A recent study reported an increase in actuation strain of free-standing corrugated PPy film in comparison to a non-corrugated film.[34] These free standing films were tested under tension where the corrugation height (parameter *H*) is likely to depend on the applied load so that the expected actuation strain is less predictable. In the present study, the PPy corrugation roughness is likely to be fixed by the underlying rubber layer and much less dependent on external loads.

A second major influence affecting actuation of the PPy/rubber composites is the restricting effect of the rubber layer on the PPy actuation. The laminated composite can be treated as the PPy actuator and rubber sheet loaded in a parallel arrangement (Figure S3). The strain in each layer is always the same, so that any actuation strain generated by the PPy will be opposed by the elastic stress generated in the rubber layer. As described in the Supporting Information, the net actuation strain expected in this case is given by:

$$\varepsilon = \frac{1}{1+r'}\left[\varepsilon_o + \varepsilon_p\left(\frac{Y}{Y'}-1\right)\right] \ldots\ldots \text{(b)}$$

where ε_o represents the free strain of neat PPy films, r' is the stiffness ratio of rubber to PPy after actuation, ε_p is the pre-strain applied before actuation and Y and Y' are the Young's moduli of PPy before and after actuation. Both neat PPy and rubber are approximated as ideal elastic materials with stiffness defined as YA/l_o, where Y, A, l_o are Young's modulus, cross-sectional area, and unloaded length, respectively. Increasing rubber roughness effectively increases the average thickness and stiffness of the rubber layer, increasing parameter r' and so reducing the actuation strain of the PPy/rubber composite actuators. With ε_p=0 equation

(b) predicts a decrease in free strain with increasing stiffness ratio *r'*. Experimentally it was observed that the PPy/rubber free strain decreased as the rubber roughness increased.

In all cases a decrease in strain occurred when a higher loading pre-strain was applied to the PPy/rubber samples (Figure 4c). It is interesting that some samples (grit size of P240 and P600) were still able to generate reasonable actuation strains (~1%) at an applied stress of 160 kPa, corresponding to 24% pre-strain. The relationship between actuation strain and applied isotonic stress has been analysed previously for neat PPy actuators.[35, 36] In these systems the change in elastic modulus of the PPy before and after actuation causes a length strain that usually opposes the inherent actuation. The analysis described by equation (b) suggests that increasing applied pre-strain/stress will decrease the actuation strain linearly. The predicted actuation strain at different loads is plotted in Figure 4c as dashed lines. Here the elastic modulus of PPy/TFSI at the initial reduced and final oxidized states were taken as Y~20 MPa and Y'~80 MPa,[37] and the bulk thickness of PPy and rubber were treated as ~24 μm and ~240 μm, respectively (taken from SEM images, Figure 3). The free strain of each case was obtained by extrapolating the strain-stress data to zero load. The experimental and calculated values agree closely in all cases except for the smoothest rubber film. PPy-coated rubber produced from the smoothest sandpaper (P1200) showed relative higher strain than the other samples but lost actuation strain more severely when the external stress increased. The difference between the measured and predicted actuation strains for this sample was perhaps due to the loss of conductivity caused by cracking in the gold layer (Figure 4a) and delamination of the PPy/gold from the rubber (Figure 3). Typical cyclic voltammograms, shown in Figure 4b, display pronounced redox peaks, but with a significantly lower current for the smoothest sample, indicating a decreased electrical conductivity.

CONCLUSIONS

Here we successfully demonstrate a simple and novel method to create stretchable PPy actuators. The PPy/rubber composite actuators can be stretched to 25% and still provide a useful actuation strain (~2%). The stretchability was accomplished by introducing a disordered corrugated structure on the rubber substrate surface. The working pre-strain range of these stretchable actuators is substantially higher compared to free standing PPy at the cost of smaller actuation strain. However, the pressures generated are considered to be adequate for providing a gentle massaging effect in a wearable sleeve. The low input voltage of PPy actuators is a major advantage of these materials in comparison to competing stretchable actuators[38,39] such as dielectric elastomers that operate at kilovolt inputs.

ACKNOWLEDGEMENTS

This research was supported by a grant from the National Breast Cancer Foundation Australia. The Australian National Fabrication Facility Materials Node is thanked for their provision of research facilities. G.M.S. and G.G.W. were supported by ARC Professorial Fellowship and ARC Laureate Fellowship, respectively. The University of Wollongong Electron Microscopy Centre is also acknowledged for scanning electron microscopy.

REFERENCES AND NOTES

1 Ino, S.; Sato, M.; Hosono, M.; Izumi, T. *Sens. Actuator B-Chem.* **2009**,*136*, 86-91,

2 Cullell, A.; Moreno, J. C.; Rocon, E.; Forner-Cordero, A; Pons, J. L; *Mech. Mach. Theory.* **2009**, *44*, 860-872.

3 Hirata, Y.; Iwano, T.; Tajika, M.; Kosuge, K. In 17th IEEE International Symposium on Robot and Human Interactive Communications, Munich, Germany, Aug 01-03, 2008; IEEE: New York, 2008.

4 Jeong, Y.; Lee, D.; Kim, K.;Park, J. In 9th IEEE International Workshop on Robot and Human Interactive Communication**,** Osaka, Japan**,** Sep 27-29, 2000; IEEE:New York,2000.

5 Sun, Y. G.; Choi, W. M.; Jiang, H. Q.; Huang, Y. G. Y.; Rogers, J. A. *Nat. Nanotechnol.* **2006**, *1*, 201-207.

6 Kim, D. H.; Ahn, J. H.; Choi, W. M.; Kim, H. S.; Kim, T. H.; Song, J. Z.; Huang, Y. G. Y.; Liu, Z. J.; Lu, C.; Rogers, J. A. *Science.***2008***, 320*, 507-511.
7 Wang, C. Y.; Zheng, W.; Yue, Z. L.; Too, C. O; Wallace, G. G. *Adv.Mater.***2011***, 23*, 3580-3584.
8 Hyun, D. C.; Park, M.; Park, C.; Kim, B.; Xia, Y.; Hur, J. H.; Kim, J. M.; Park, J. J.; Jeong, U. *Adv.Mater.***2011**, *23*, 2946-2950.
9 Lee, J.; Wu, J. A.; Shi, M. X.; Yoon, J.; Park, S. I.; Li, M.; Liu, Z. J.; Huang, Y. G.; Rogers, J. A. *Adv.Mater.* **2011**,*23*, 986-991,
10 Hu, L. B.; Pasta, M.; La Mantia, F.; Cui, L. F.; Jeong, S.; Deshazer, H. D.; Choi, J. W.; Han, S. M.; Cui, Y. *Nano Lett.***2010***, 10*, 708-714.
11 Kaltenbrunner, M.; Kettlgruber, G.; Siket, C.; Schwodiauer, R.; Bauer, S. *Adv.Mater.* **2010***, 22*, 2065-2067.
12 Pelrine, R.; Kornbluh, R.; Pei, Q. B.; Joseph, J. *Science.***2000***, 287*, 836-839.
13 Huang, H. B.; Spaepen, F. *Acta Mater.***2000***, 48*, 3261-3269.
14 Bowden, N.; Brittain, S.; Evans, A. G.; Hutchinson, J. W.; Whitesides, G. M. *Nature.***1998**, *393*, 146-149.
15 Sun, Y. G.; Kumar, V.;Adesida, I.; Rogers, J. A. *Adv.Mater.***2006***, 18*, 2857-2862.
16 Wang, X. L.; Hu, H.; Shen, Y. D.; Zhou, X. C. ;Zheng, Z. J. *Adv.Mater.***2011***, 23*, 3090-3094.
17 Lacour, S. P.; Wagner, S.; Huang, Z. Y.; Suo, Z. *Appl. Phys. Lett.* **2003**,*82*, 2404-2406.
18 Khang, D. Y.; Jiang, H. Q.; Huang, Y. ;Rogers, J. A; *Science.***2006**, *311*, 208-212.
19 De Rossi, D.; Della Santa, A.; Mazzoldi, A. *Mater. Sci. Eng. C-Biomimetic Supramol. Syst.* **1999**,*7*, 31-35.
20 Campbell, T. E.; Munro, B. J.; Wallace, G. G. ; Steele, J. R. *J. Biomech.* **2007**,*40*, 3056-3059.
21 Tjahyono, A. P.; Aw, K. C. ; Travas-Sejdic, J. *Sens. Actuator B-Chem.* **2012**,*166*, 426-437,
22 Baughman, R. H. *Synth. Met.***1996***,78*, 339-353.
23 Brochu, P .Pei, Q. *Macromol.Rapid Commun.* **2010**, *31*, 10-36.
24 Smela, E. *Adv. Mater.***2003***, 15*, 481-494.
25 Murray, P.; Spinks, G. M.; Wallace, G. G.; Burford, R. P. *Synth.Met.***1998***,97*, 117-121.
26 Madden J.D; Rinderknecht D.;Anquetil P.A; Hunter I.W. *Sens. Actuator A-Phys.***2007***, 133*, 210-217.
27 Ding, J.; Liu, L.; Spinks, G. M.; Zhou, D.; Wallace, G. G.; Gillespie, J. *Synth. Met.***2003***, 138*, 391-398.
28 Otero, T. F.; Cascales, J. J. L. ; Arenas, G. V. *Mater. Sci. Eng. C-Biomimetic Supramol.Syst.* **2007***, 27*, 18-22.
29 Ko, D. S. C.; Lerner, R.; Klose, G.; Cosimi, A. B. *Arch. Surg.* **1998***, 133*, 452-457.
30 Johansson, K.; Lie, E.; Ekdahl, C.; Lindfeldt, J. *Lymphology,* **1998***, 31*, 56-64.
31 Hutchison, A. S.; Lewis, T. W.; Moulton, S. E.; Spinks, G. M. ; Wallace, G. G. *Synth.Met.***2000***, 113*, 121-127.
32 Bay, L.;West, K.; Sommer-Larsen, P.;Skaarup, S. ; Benslimane, M. *Adv. Mater.***2003***, 15*, 310-313.
33 Hara, S.; Zama, T.; Takashima, W.; Kaneto, K. *Polym. J.***2004***, 36*, 933-936.
34 Morita, T.; Chida, Y.; Hoshino, D.; Fujiya, T. ; Nishioka, Y. *Mol. Cryst. Liquid Cryst.* **2010**,*519*, 121-127.
35 Spinks, G. M.; Liu, L.; Zhou, D.; Wallace, G. G. *Adv. Funct. Mater.***2002***,12*, 437-440.
36 Spinks, G. M. ;Truong, V.-T. *Sens. Actuator A-Phys.***2005***, 119*, 455-461.
37 Zheng, W. *Analysis of high performance polypyrrole actuators.* Ph.D thesis, University of Wollongong, Wollongong, N.S.W, July 2011.
38 Pelrine, R.; Kornbluh, R.; Pei, Q.; Joseph, J. *Science* **2000,** *287*, 836-839.
39 Carpi, F.; Frediani, G.; Turco, S.; De Rossi, D. *Adv. Funct. Mater.* **2011,** *21*, 4152-4158.

FIGURE CAPTIONS

FIGURE 1. Schematic illustration of the process used to fabricate stretchable PPy/rubber actuators.

FIGURE 2. SEM images of rubber sheets without/with PPy coatings; a)-d): gold coated rubber, obtained from grit sizes of P120 (125 μm), P240 (58.5 μm), P600 (25.8 μm) and P1200 (15.3 μm); a')-d'): corresponding rubber with PPy coatings; scale bars represent 100 μm.

FIGURE 3. Cross section images of PPy/gold/rubber. a)~d), grit size P120 (125 μm), P240 (58.5 μm), P600 (25.8 μm) and P1200 (15.3 μm). Note the different scale bars in a) and b) compared with c) and d).

FIGURE 4. a) Variation of the normalized change in electrical resistance of gold-coated roughened rubber with applied tensile strain. b) Typical CVs of PPy-coated rubber band when stretched and c) typical isotonic actuation strain; d) isometric pressure generated by PPy on roughened rubber;

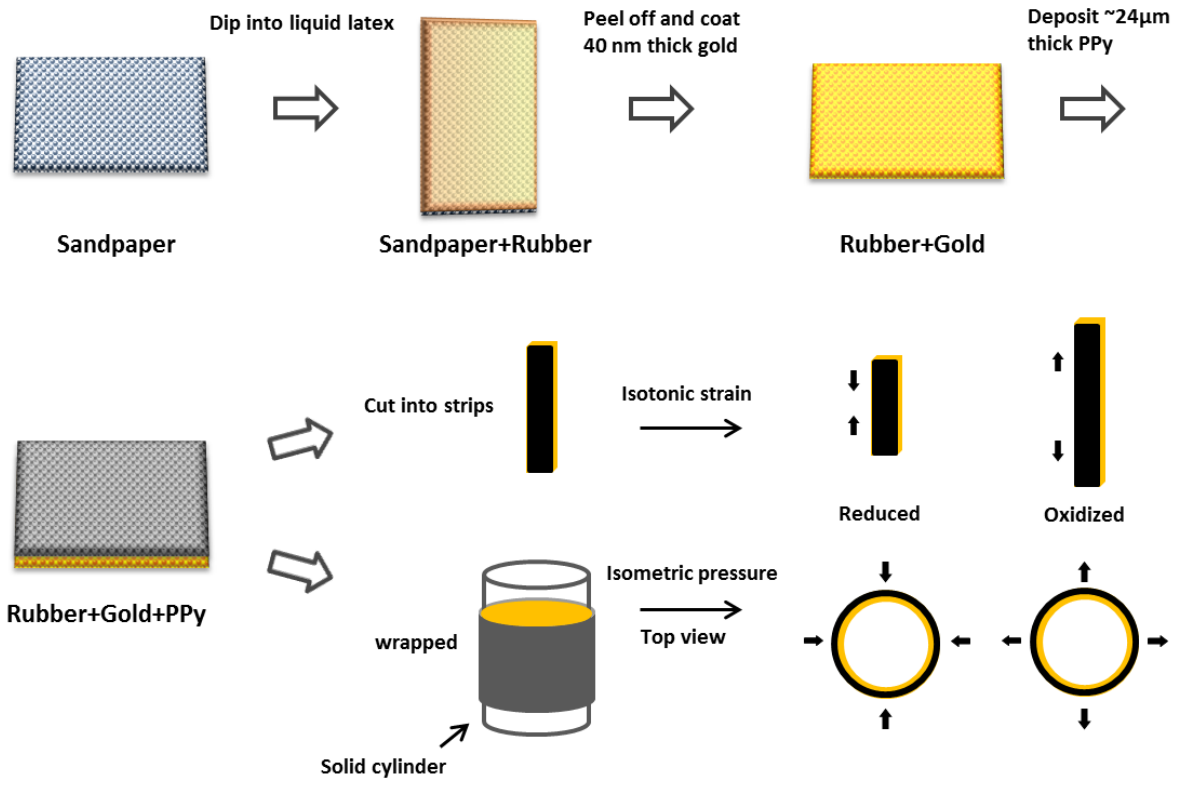
Dip into liquid latex
Peel off and coat
40 nm thick gold
Deposit ~24µm
thick PPy
Sandpaper
Sandpaper+Rubber
Rubber+Gold
Cut into strips
Isotonic strain
Reduced
Oxidized
Rubber+Gold+PPy
wrapped
Isometric pressure
Top view
Solid cylinder

Figure 1

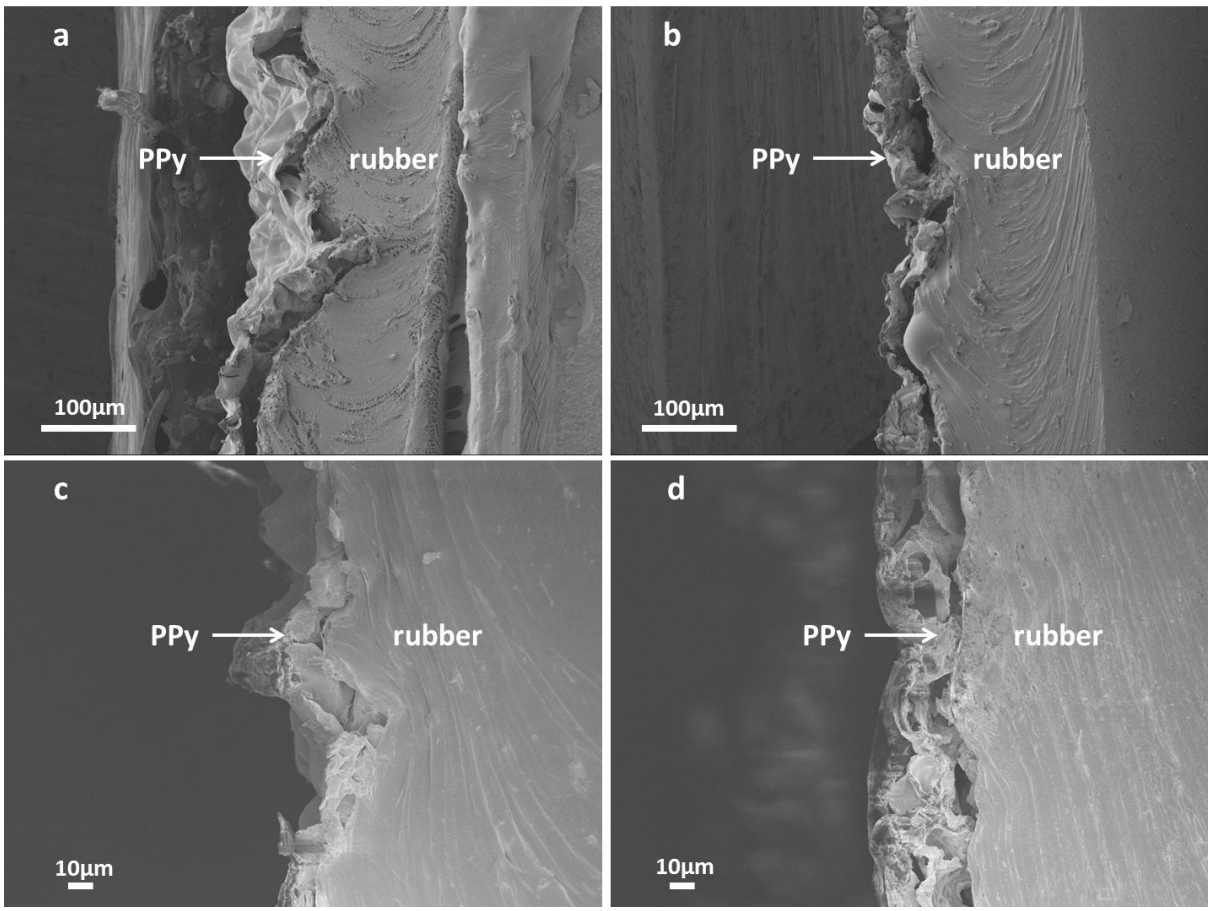
a
PPy
rubber
100µm
b
PPy
rubber
100µm
c
PPy
rubber
10µm
d
PPy
rubber
10µm

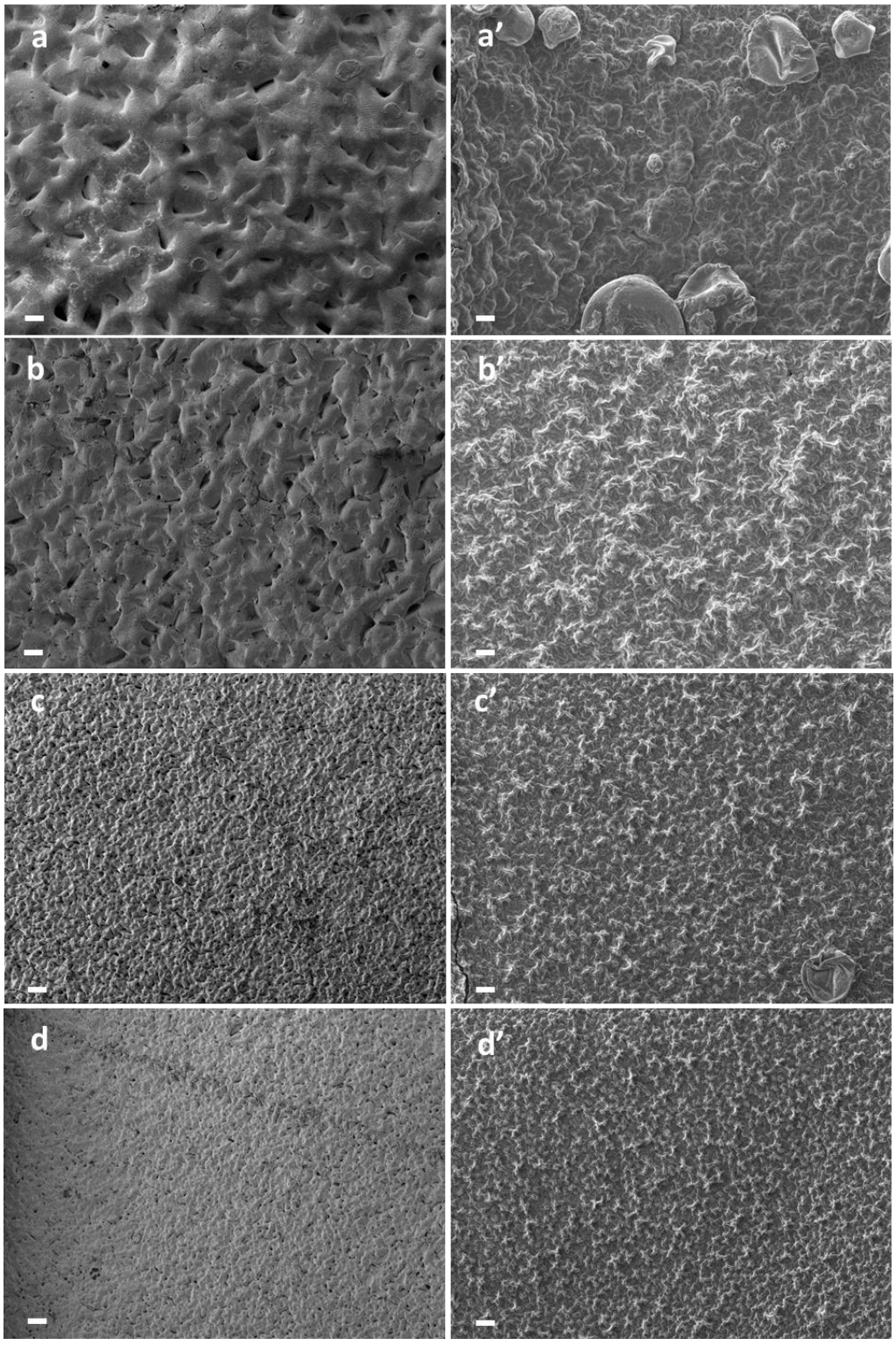

Figure 2

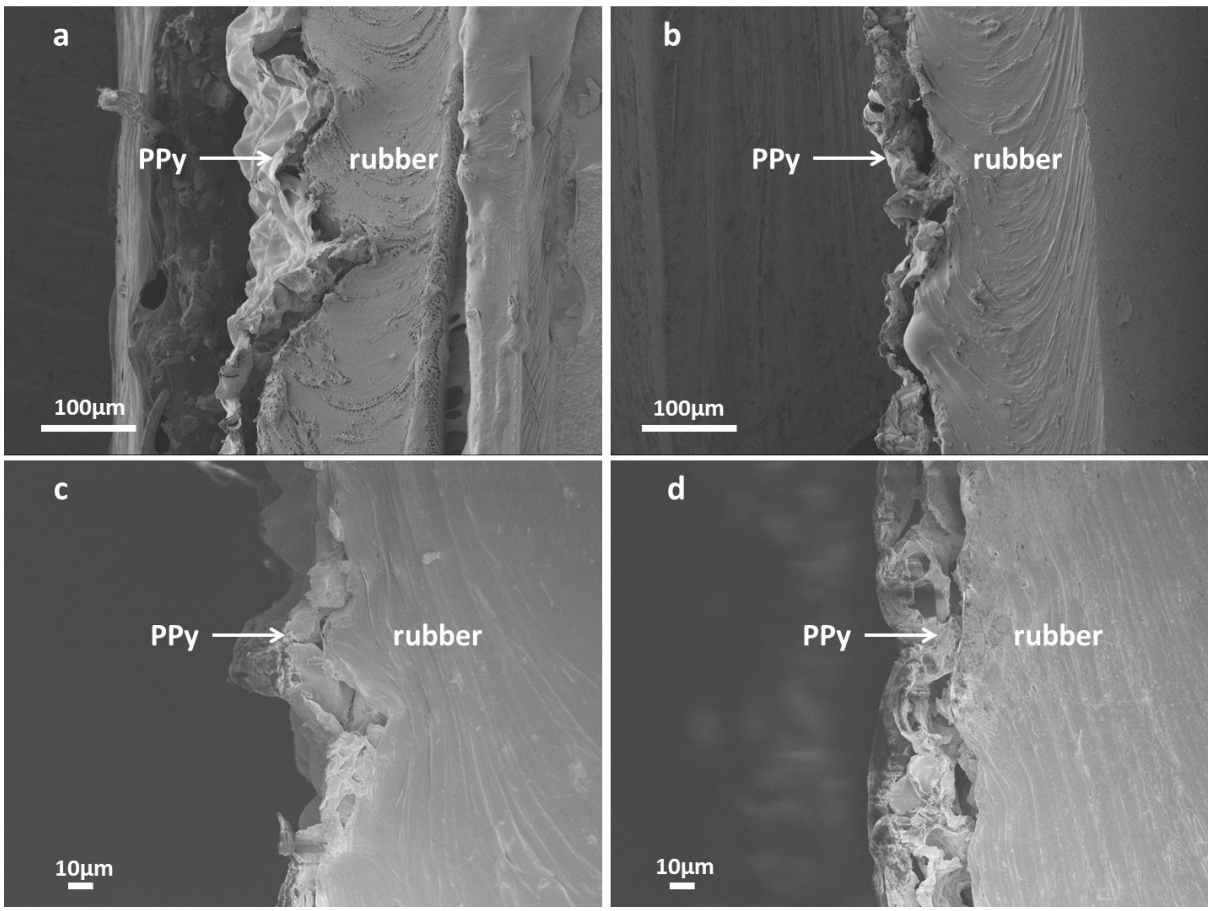
a
PPy
rubber
100µm
b
PPy
rubber
100µm
c
PPy
rubber
10µm
d
PPy
rubber
10µm

Figure 3

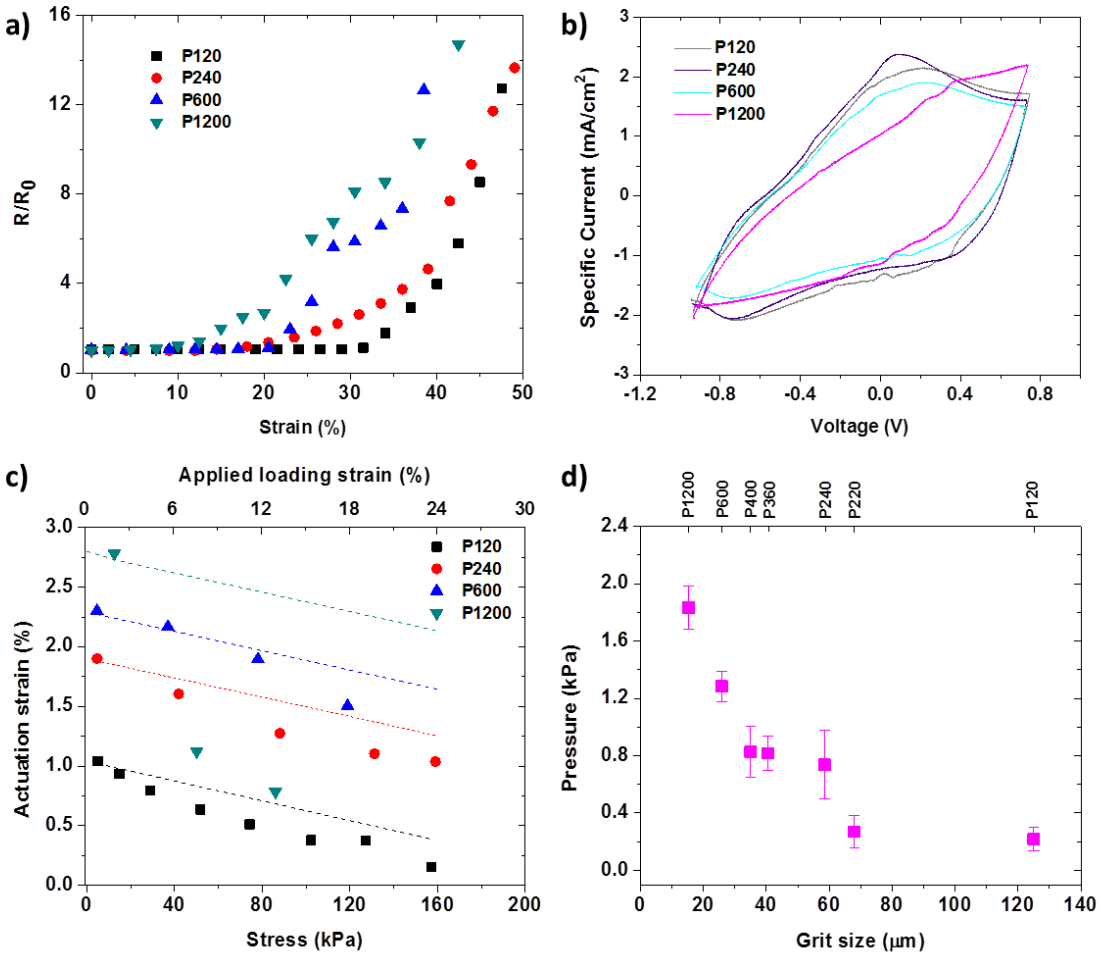
a)
R/R0
Strain (%)
P120
P240
P600
P1200
b)
Specific Current (mA/cm2)
Voltage (V)
P120
P240
P600
P1200
c)
Applied loading strain (%)
Actuation strain (%)
Stress (kPa)
P120
P240
P600
P1200
d)
P1200
P600
P400
P360
P240
P220
P120
Pressure (kPa)
Grit size (μm)

Figure 4

Supporting Information

1. SEMs of gold coated rubber after stretching.

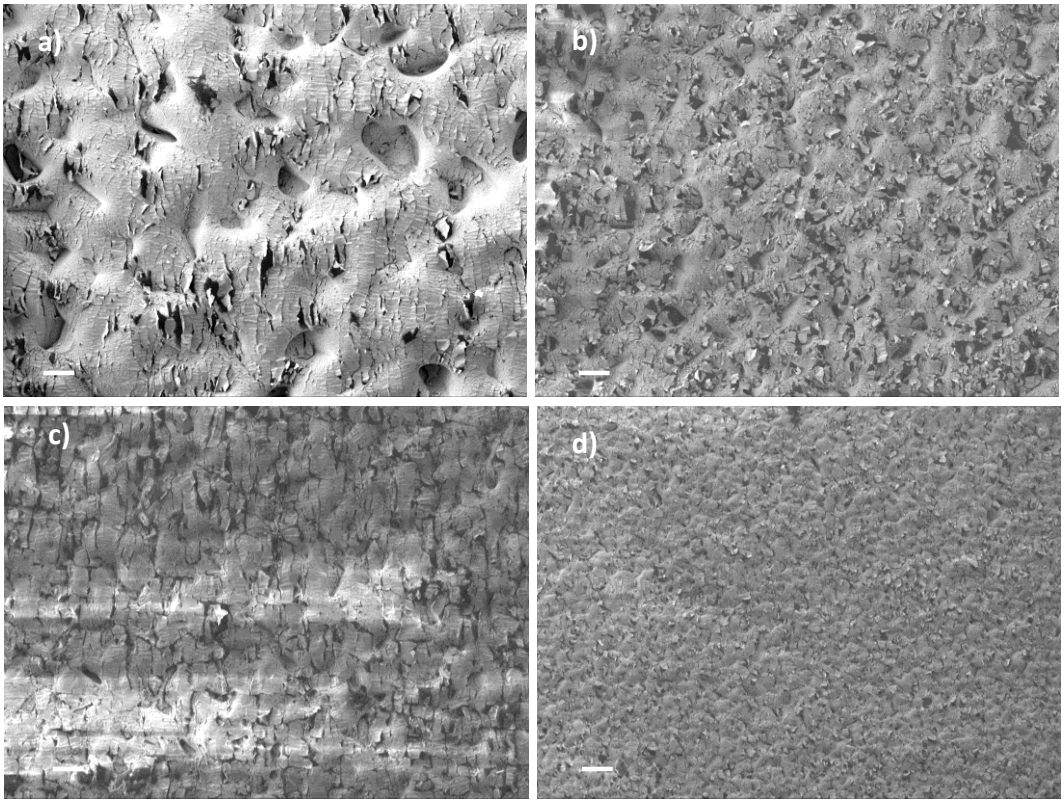

Figure S1. SEM images of gold coated rubber after stretching to 50% of strain; a)-d): grit sizes of P120 (125 µm), P240 (58.5 µm), P600 (25.8 µm) and P1200 (15.3 µm); scale bars represent 100 µm.

Gold coated rubber were stretched to 50% of strain and then released to their original length. Cracks on the metal layers were formed and ran perpendicular to the elongation direction. These cracks in the metal layers are thought to be the main reason for the increase in resistance of the metal-coated rubbers when stretched to high strains.

2. Derivation of equation (a):

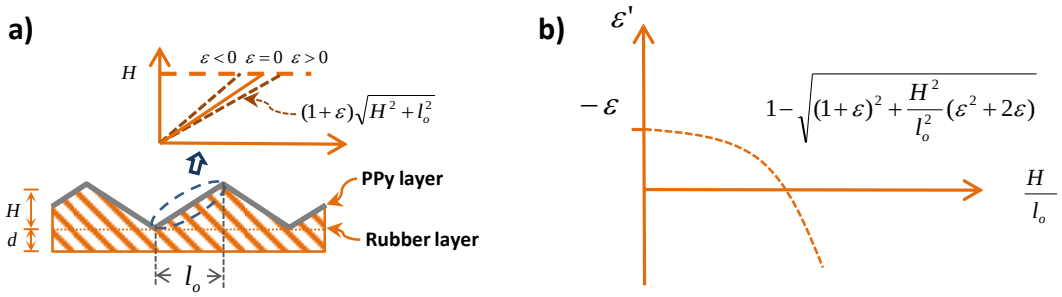

Figure S2. Simplified model of PPy on roughened rubber. The rubber roughness is treated as a triangle wave so that the PPy length becomes the long side of the triangle in part a).

For an ideal corrugated structure simplified as a triangle wave and assuming that the thickness of the PPy layer is comparable to the surface roughness, the total length of PPy can be written as:

$$\sqrt{H^2 + l_o^2}$$

For a given sample length l_o and parameter H related to the sample roughness, the total length of PPy changes to:

$$(1+\varepsilon)\sqrt{H^2 + l_o^2}$$

when actuated and the PPy generates an actuation strain ε.

The length change of PPy projected on the axis parallel to the sheet direction is:

$$\sqrt{(1+\varepsilon)^2(H^2 + l_o^2) - H^2}$$

by assuming roughness does not change during actuation.

Hence, the length change for a given band can be written as:

$$l_o - \sqrt{(1+\varepsilon)^2(H^2 + l_o^2) - H^2}$$

and actuation strain ε' of corrugated PPy is:

$$\varepsilon' = 1 - \sqrt{(1+\varepsilon)^2 + \frac{H^2}{l_o^2}(\varepsilon^2 + 2\varepsilon)} \quad \ldots\ldots \text{(a)}$$

Note that actuation strain ε' and ε might be positive or negative, representing elongation or contraction of actuation.

2. Derivation of equation (b):

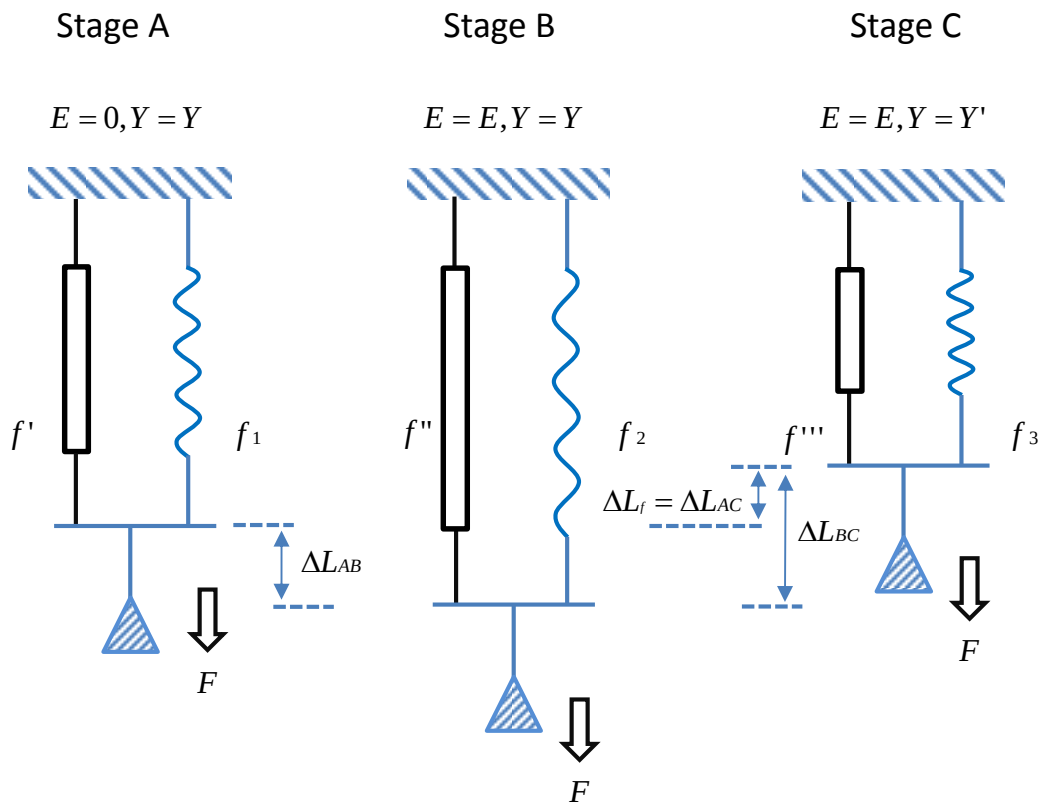

Figure S3. Length changes occurring during the loading and actuation process for an actuator working parallel to a spring. *E* is the applied electrical potential and *Y* is the actuator material's Young's modulus.

A PPy/rubber system can generally be treated as an actuator paralleled to a spring working against a constant load. The overall actuation stroke is determined by a combination of the voltage-induced shape change in the PPy and the change in length due to the applied

force. The actuator stroke is first estimated for the case where the stiffness of the PPy does not change when the voltage is applied (from stage A to stage B in Figure S3):

$$\Delta L_{AB} = \Delta L_0 + \frac{f''-f'}{k_{PPy}} \ldots\ldots (1)$$

The second contribution to the actuator stroke occurs when the stiffness of the PPy changes due to the evolving of PPy's elastic modulus when a voltage is applied (from Stage B to Stage C in Figure S3):

$$\Delta L_{BC} = \frac{f'''}{k_{PPy}'} - \frac{f''}{k_{PPy}} \ldots\ldots (2)$$

Hence, the isotonic actuation stroke (ΔL_f) can be given by the sum of three parts: free stroke of neat PPy films (ΔL_o), displacement caused by an increasing spring force ($\frac{f''-f'}{k_{PPy}}$), and displacement caused by a change in modulus ($\frac{f'''}{k_{PPy}'} - \frac{f''}{k_{PPy}}$):

$$\Delta L_f = \Delta L_o + \frac{f''-f'}{k_{PPy}} + (\frac{f'''}{k_{PPy}'} - \frac{f''}{k_{PPy}}) \ldots\ldots (3),$$

where k_{PPy} and k'_{PPy} stand for stiffness of PPy before and after voltage is applied. $f' \sim f'''$ is the force evolution of PPy at different stages, $f_1 \sim f_3$ represents the force applied on rubber from stage A to stage C. The initial force f' applied on PPy equals $k_{PPy}\Delta L_o'$, representing the pre-load stroke ($\Delta L_o'$) induced force.

In the isotonic condition, the total force of the whole system remains constant, so now we have:

$$f' + f_1 = f''' + f_3 \ldots\ldots (4)$$

and

$$f_1 = f_3 - k_{rubber}\Delta L_f \ldots\ldots (5)$$

Therefore, the final force applied to PPy is $f''' = f' - k_{rubber}\Delta L_f$. Combining equations (1)-(5), the isotonic actuation strain (ε) can be given by:

$$\varepsilon = \frac{1}{1+r'}\left[\varepsilon_o + \varepsilon_p\left(\frac{Y}{Y'} - 1\right)\right] \ldots\ldots \text{(b)},$$

in which ε_o indicates 'free strain' of a free standing PPy actuator, ε_p stands for the stepwise increased force induced pre-strain applied to the bilayer system. The free strain ε_0 and stiffness ratios (r') are constant values and usually $Y/Y' < 1$, as the elastic modulus of PPy is larger at the oxidized state (Y') compared with the reduced state (Y).[1] The result is that the isotonic actuation strain is expected to decrease with increasing tensile pre-strain.

References:

1. Otero, T. F.; Cascales, J. J. L.; Arenas, G. V. *Mater. Sci. Eng. C-Biomimetic Supramol.Syst.* **2007**, *27*, 18-22.